other planetary bodies where fluid flow establishes gradients in redox potential, as long as there are sources of required nutrients, water, and carbon.

References and Notes

1. R. J. Parkes *et al.*, *Nature* **371**, 410 (1994).
2. D. R. Lovely and F. H. Chapelle, *Rev. Geophys.* **33**, 365 (1995); S. V. Liu *et al.*, *Science* **277**, 1106 (1997); C. Zhang *et al.*, *Geochim Cosmochim. Acta* **61**, 4621 (1997).
3. T. O. Stevens and J. P. McKinley, *Science* **270**, 450 (1995); I. H. Thorseth, H. Furnes, M. Heldal, *Geochim. Cosmochim. Acta* **56**, 845 (1992).
4. I. H. Thorseth, I. Torsvik, H. Furnes, K. Muehlenbachs, *Chem. Geol.* **126**, 137 (1995); H. Furnes, I. Thorseth, O. Tumyr, T. Torsvik, M. Fisk. *Proc. Ocean Drill. Program Sci. Results* **148**, 191 (1996); S. J. Giovannoni, M. R. Fisk, T. D. Mullins, H. Furnes, *ibid.*, p. 207.
5. T. Torsvik, H. Furnes, K. Muehlenbachs, I. H. Thorseth, O. Tumyr, *Earth Planet. Sci. Lett.*, in press; M. R. Fisk, S. J. Giovannoni, T. D. Mullins *Eos (Fall Meet. Suppl.)* **75**, 706 (1994).
6. M. R. Fisk, S. J. Giovannoni, E. Urbach, I. H. Thorseth, *Eos (Fall Meet. Suppl.)* **78**, 740 (1997).
7. R. Huber, P. Stoffers, J. L. Cheminee, H. H. Richnow, K. O. Stetter, *Nature* **345**, 179 (1990).
8. R. M. Haymon *et al.*, *Earth Planet. Sci. Lett.* **119**, 85 (1993); S. K. Juniper, P. Martineau, J. Sarrazin, J. Y. Gélinas, *Geophys. Res. Lett.* **22**, 179 (1995); C. D. Taylor and C. O. Wirsen, *Science* **277**, 1483 (1997).
9. I. H. Thorseth, H. Furnes, O. Tumyr, *Chem. Geol.* **119**, 139 (1995).
10. J. L. Crovisier, J. Honnorez, J. P. Eberhart, *Geochim. Cosmochim. Acta* **51**, 2977 (1987); G. Berger, C. Claparols, C. Guy, V. Daux, *ibid.* **58**, 4875 (1994).
11. Sea floor surface samples were collected by dredges and submersibles from seamounts and mid-ocean ridges. Buried samples were collected during the Deep Sea Drilling Project and the Ocean Drilling Program.
12. NSF and the Joint Oceanographic Institutions supported this work. Samples are from the Ocean Drilling Program sample repositories and from D. Graham, D. Christie, R. Embley, and M. Perfit. The photomicrographs were taken with Nikon and Leica microscopes, which were loaned by D. Graham and F. Moore.

9 March 1998; accepted 30 June 1998

A 3000-Year Climatic Record from Biogenic Silica Oxygen Isotopes in an Equatorial High-Altitude Lake

M. Rietti-Shati, A. Shemesh,* W. Karlen

A record of oxygen isotopes in biogenic opal, 4200 to 1200 calibrated years before the present, from a high-altitude proglacial lake on Mount Kenya, East Africa, exhibits short-term fluctuations on a time scale of centuries as well as long-term variations. The short-term fluctuations are attributed to changes in the glacier meltwater input, and the long-term variations are related to changes in lake temperature. The record indicates that the climate was warm in Equatorial East Africa from 2300 to 1500 years before the present.

The Holocene, although relatively more stable than the Late Pleistocene, was also subject to abrupt climatic changes (*1, 2*). Small, low-latitude glaciers are especially sensitive to such climatic changes (*3*). Mount Kenya, in East Africa, is a dormant volcano that contains several small glaciers and lakes located at an elevation of 4200 to 5200 m (Fig. 1). In 1978 two ice cores were retrieved from the col (4870 m) between the Lewis and Gregory glaciers on Mount Kenya (Fig. 1). However, the lack of a clear relation between air temperature and the isotopic composition of the ice hampered detection of climatic signals (*4*). Karlen and Rosqvist (*5*) investigated the sediments from Hausberg Tarn, a proglacial lake, to study glacier fluctuations on Mount Kenya (0°10′S 37°20′E; Fig. 1). X-ray radiography of the cores, together with changes in organic content, indicates that there has been a succession of glacier advances and retreats during the past 4000 years (*5*). These findings are qualitative because the high-altitude lakes in East Africa are void of the carbonate material (*6*) that is commonly used for isotopic studies of climate change. On the other hand, these lakes contain biogenic opal that is suitable for isotopic analysis. Here we report oxygen isotope measurements of biogenic opal from Hausberg Tarn.

The climate of East Africa is affected by the seasonal position of the intertropical convergence zone and regional factors associated with lakes, topography, and maritime influence (*7*). The lower tropospheric flow over East Africa comes predominantly from the southeast, and, because of the topographic control, maximum rainfall occurs at intermediate elevations (2500 to 3000 m) on the southern and eastern flanks of Mount Kenya (*5*). Above 4500 m, most of the annual precipitation (700 to 800 mm) falls as snow. Temperatures average about 0°C (*4, 5*) and are lowest in March and April and highest in July and August.

We obtained a 180-cm-long sediment core from Hausberg Tarn in 1996 (Fig. 1). The top part of the core, containing the most recent sediment was too soft, and could not be retrieved by our coring device. The lake (area, 12,000 m^2; 10 m at the deepest part) is located near the moraines of Cesar and Joseph Glaciers (Fig. 1) and its sediments contain both authigenic opal produced by diatoms and allochthonous material derived from the surrounding steep mountain slopes (*5*). Diatoms are photosynthetic algae that secrete opal ($SiO_2 \cdot nH_2O$) as an internal shell with a known isotopic fractionation between the opal and the water. The temperature dependency of the opal-water fractionation is given by

$$t°\mathrm{C} = 11.02 - 2.04(\delta^{18}O_{si} - \delta^{18}O_{w} - 40) \qquad (1)$$

where t is the water temperature and $\delta^{18}O_{si}$ and $\delta^{18}O_{w}$ are the isotopic compositions of opal and water, respectively (*8–11*). Thus, the measurement of $\delta^{18}O_{si}$ provides information both about the lake temperature and about the $\delta^{18}O_{w}$ of the lake in the past (*12*).

In 1997 we analyzed water samples from the lake, from surrounding streams, and from rainwater collected at Mackinder camp (located at an altitude of 4200 m) to determine the composition of the water flowing to the lake today. The isotopic composition of all water samples was measured by standard techniques for $\delta^{18}O$ and $\delta^{2}H$. Eight ^{14}C accelerator mass spectrometry dates on bulk organic matter of the core (*13*) indicate that the average sediment accumulation was 0.62 mm/year (Fig. 2A).

The $\delta^{18}O$ values of the lake's surface and deep water are both −6.3 per mil and indicate that the lake is not stratified. Therefore, diatom $\delta^{18}O_{si}$ values represent the whole water volume despite the fact that most of the fossil diatoms are bottom dwellers. Although Hausberg Tarn has an outlet to Oblong Tarn (Fig. 1), whose $\delta^{18}O_{w}$ value is −6.4 per mil, it has no visible inlet. The lake $\delta^{18}O_{w}$ is similar to the $\delta^{18}O_{w}$ value of the Lewis Glacier meltwater stream (−6.2 per mil) and also to the overall average $\delta^{18}O$ of the Lewis Glacier ice cores (*4*) (10-m-long cores). Because of their geographic proximity and similar altitude (Fig. 1), we assume that the Cesar and Josef Glaciers have $\delta^{18}O$ values similar to that of the Lewis Glacier. The rainwater $\delta^{18}O_{w}$ values obtained from Mackinder camp (4200 m) are −0.6 and −1.4 per mil. Thus, we conclude that Hausberg Tarn is a through-flow

---

M. Rietti-Shati and A. Shemesh, Department of Environmental Sciences and Energy Research, Weizmann Institute of Science, Rehovot 76100, Israel. W. Karlen, Department of Physical Geography, University of Stockholm, Stockholm S-106 91, Sweden.

*To whom correspondence should be addressed.

lake replenished primarily by high-altitude glacier meltwater, rather than by rainfall, and that evaporation has a negligible effect. The $\delta^{18}O_w$ value of a small stream close to Hausberg Tarn, −3.5 per mil, suggests that this source does not make a significant contribution to the water budget of the lake.

The diatom $\delta^{18}O_{si}$ record (Fig. 2B) ranges from 4200 to 1200 years before the present (calibrated; cal yr B.P.) (*13*). It shows short-term fluctuations on the order of about 2 per mil on a time scale of centuries. A five-point running average shows that the lower part of the record (4200 to 2500 cal yr B.P.; average $\delta^{18}O_{si}$ of 34.5 per mil) has a $\delta^{18}O_{si}$ value higher by about 2 per mil relative to the upper part (2100 to 1500 cal yr B.P.), whereas the uppermost part (1500 to 1200 cal yr B.P.) has intermediate $\delta^{18}O_{si}$ values that are close to those of 2500 to 2200 cal yr B.P. The isotopic shifts centered at 2200 and 1500 cal yr B.P. occur during intervals shorter than 300 years.

The surface lake temperature was about 7°C during summer 1997. This value, along with the lake $\delta^{18}O_w$ value of −6.3 per mil, cannot be used for the interpretation of our $\delta^{18}O_{si}$ measurements in terms of absolute temperature and $\delta^{18}O_w$ because the top of the core is 1200 years older than the present-day water and calibration of lacustrine opal-water fractionation has not yet been performed. Therefore, we discuss the record in terms of relative temperature and $\delta^{18}O_w$ variations rather than absolute values.

The isotopic changes in diatom $\delta^{18}O_{si}$ can be interpreted as changes in lake water temperature or as changes in $\delta^{18}O_w$ or both. The high-frequency fluctuations cannot be attributed solely to temperature variations, because this would require that a change of more than 5°C (Eq. 1), and in one case 10°C, occurred within 50 to 100 years. Therefore, some part of these fluctuations must be due to short-term changes in the $\delta^{18}O$ of the meltwater input. The most plausible explanation for the short-term depleted $\delta^{18}O_{si}$ values is melting of the top 1 to 2 m of the glacier ice, because the $\delta^{18}O$ values in the upper part of the Lewis ice cores (*4*) are variable and depleted by up to 5 per mil relative to the subsurface (−10 per mil in the upper 1 m and −5 per mil in the subsurface).

Our $\delta^{18}O_{si}$ record is characterized by two rather different isotopic states, 4200 to 2300 cal yr B.P. and 2100 to 1500 cal yr B.P. The shift between these two states may represent either a change in the average $\delta^{18}O$ value of the glacier ice, which determines the $\delta^{18}O_w$ value of the lake inflow, or a change in surface temperatures on Mount Kenya.

A decrease in $\delta^{18}O$ of 1 per mil can be interpreted as either a 0.9°C decrease in the temperature of precipitation formation or a 2°C increase in the temperature of the source (*14, 15*). If the latter were the cause of the Mount Kenya glacier $\delta^{18}O$ depletion, a warming of 4°C in the moisture source, the Indian Ocean surface water, would have been expected to occur before 2300 yr B.P. However, recent studies do not support this scenario. Alkenone paleothermometry (*16*) of sediment cores recovered from the tropical Indian Ocean (20°N to 20°S) reveals a minor cooling trend of about 0.5°C from 5000 to 1000 yr B.P. Possible warming of the surface water of the Arabian Sea is suggested by weakening of the southwest monsoon-induced upwelling since 5000 cal yr B.P. (*17*) but the Arabian Sea is not considered the main source of moisture for the precipitation on Mount Kenya.

The most prominent feature of the ice cores recovered in Mount Kenya (*4*) is the homogeneity of $\delta^{18}O$ values below the surface of the glacier. It is caused by melting and percolation (*3*) and reflects the long-term averaging of these effects. The present Lewis Glacier contains ice of the past 500 years. Therefore it can be assumed that the average $\delta^{18}O$ value of glaciers is inert and cannot change over periods of a few centuries. We conclude that the shift to more depleted $\delta^{18}O_{si}$ values between 2300 and 2000 cal yr B.P. occurred during an interval that was too short to allow for any major change in the average $\delta^{18}O$ value of the glacier. Thus, according to Eq. 1, the shift to the more depleted values indicates a warming phase of up to 4°C

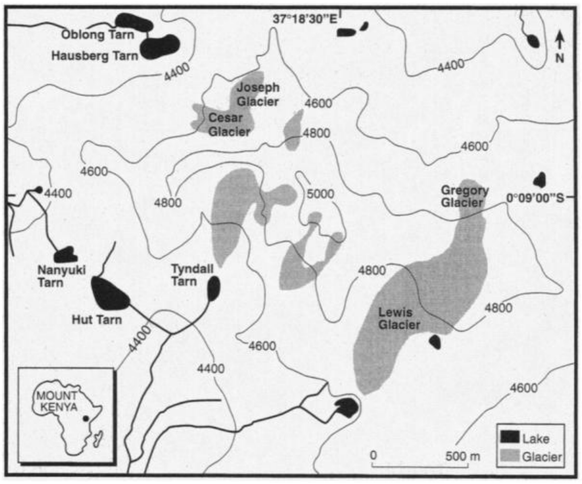

Fig. 1. Glaciers and lakes on Mount Kenya.

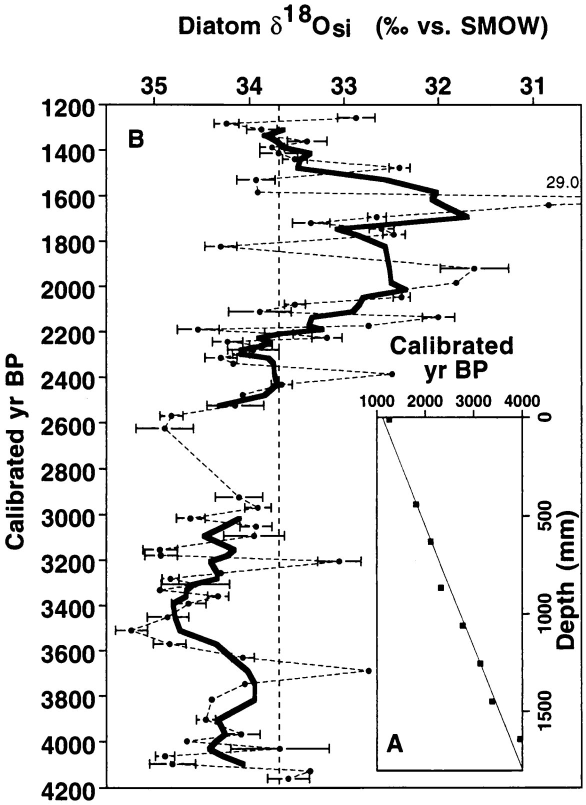

Fig. 2. (**A**) Age-depth relationship for the Hausberg Tarn sediment core. Calibrated yr B.P. were obtained from ^{14}C data according to (*20*). (**B**) Hausberg Tarn oxygen isotopic composition of diatom opal $\delta^{18}O_{si}$ (dashed line) and a five-point running mean (thick line). Error bars indicate the standard error of multiple analyses. The horizontal dashed line signifies the average $\delta^{18}O_{si}$ of the whole core. The gap from 2900 to 2700 cal yr B.P. is due to the loss of four consecutive opal samples during analytical processing.

on Mount Kenya. The $\delta^{18}O_{si}$ temperature signal could have been enhanced by the contribution of more depleted meltwater because of increased melting of the top part of the glacier.

The climatic transition around 2200 ^{14}C cal yr B.P. in our record (Fig. 2B) is also apparent in records from the equatorial part of Lake Victoria (*18*) (0°05′0″N, 32°48′2″E) and a high-altitude mire on Mount Satima, Kenya (*19*) (0°18′S, 36°35′E; 3670 m). A warm period occurring at the same time interval (about 2400 to 1250 calendar yr B.P.) has been recorded by glacier recessions on Mount Kenya (*5*) and in the northeastern St. Elias Mountains in southern Yukon Territory and Alaska and in Swedish Lapland (*1*).

This work demonstrates that sedimentary records of $\delta^{18}O_{si}$ from high-altitude lakes complement ice-core data and provide a unique isotopic archive related to climatic changes.

References and Notes

1. G. H. Denton and W. Karlen, *Quat. Res.* **3**, 155 (1973).
2. G. Bond *et al.*, *Science* **278**, 1257 (1997).
3. S. Hastenrath, *Climate Dynamics of the Tropics* (Atmospheric Sciences Library, Kluwer Academic, Dordrecht, 1991), vol. 8.
4. L. G. Thompson, *Ice Core Studies from Mt. Kenya, Africa, and Their Relationship to Other Tropical Ice Core Studies, Sea Level, Ice, and Climatic Change* (IAHS, Canberra, 1979), vol. 131, pp. 55–62.
5. W. Karlen and G. Rosqvist, *Natl. Geogr. Res.* **4**, 219 (1988).
6. F. A. Street-Perrott *et al.*, *Science* **278**, 1422 (1997).
7. S. E. Nicholson, in *The Limnology, Climatology and Paleoclimatology of the East African Lakes*, T. C. Johnson and E. C. Odada, Eds. (Gordon and Breach, Amsterdam, 1996), pp. 25–56.
8. $\delta^{18}O$ is defined by $\{[(^{18}O/^{16}O)_{sample}/(^{18}O/^{16}O)_{standard}] - 1\} \times 1000$ and is expressed in per mil.
9. A. Juillet-Leclerc and L. Labeyrie, *Earth Planet. Sci. Lett.* **84**, 69 (1987).
10. A. Shemesh, C. D. Charles, R. G. Fairbanks, *Science* **256**, 1434 (1992).
11. A. Shemesh, L. H. Burckle, J. D. Hays, *Paleoceanography* **10**, 179 (1995).
12. Diatoms were separated from the sediment and prepared for isotopic analysis by sieving, differential settling, and chemical cleaning. The isotopic determination of $\delta^{18}O_{si}$ includes partial isotopic exchange under controlled conditions followed by extraction of oxygen by fluorination (*11*). The results are calibrated versus the NBS-28 quartz international standard and reported versus SMOW. Long-term reproducibility for duplicate $\delta^{18}O_{si}$ diatom samples is 0.14 per mil, the same as for the NBS-28 standard.
13. Supplementary material is available at www.sciencemag.org/feature/data/980568.shl.
14. L. Merlivat and J. Jouzel, *J. Geophys. Res.* **84**, 5029 (1979).
15. J. Jouzel and L. Merlivat, *ibid.* **89**, 11749 (1984).
16. E. Bard, F. Rostek, C. Sonzogni, *Nature* **385**, 707 (1997).
17. P. D. Naidu and B. A. Malmgren, *Paleoceanography* **11**, 129 (1996).
18. J. C. Stager, B. Cumming, L. Meeker, *Quat. Res.* **47**, 81 (1997).
19. F. A. Street-Perrott and R. A. Perrott, *Nature* **343**, 607 (1990).
20. M. Stuiver and P. J. Reimer, *Radiocarbon* **35**, 215 (1993).

21. We thank M. Faure, Y. Cohen-Boulakia, and R. Yam for help in opal analyses; P. Boden for diatom characterization; and A. Kaufman for reviewing an early version of the manuscript.

5 February 1998; accepted 30 June 1998

Magnetic Field Effect on Picosecond Electron Transfer

P. Gilch, F. Pöllinger-Dammer, C. Musewald, M. E. Michel-Beyerle,* U. E. Steiner

The recombination dynamics of a transition metal redox system monitored by femtosecond pump-probe spectroscopy are shown to be sensitive to high magnetic fields at times shorter than 10 picoseconds. The effect, based on coherent population beats of different spin states, is quantitatively accounted for and allows direct access to spin relaxation rates far beyond the time resolution of the fastest electron paramagnetic resonance technique. The presence of this ultrafast magnetic field effect helps in understanding complex reaction schemes in transition metal chemistry, which occur in a wide range of fields, such as bioinorganic chemistry and catalysis.

Magnetic field effects on the kinetics of radical pair (RP) recombination processes are well-established phenomena in molecular photochemistry (*1*). These effects are based on the principle of spin conservation in elementary chemical reactions and on the hyperfine and Zeeman interactions that affect the spin states of the RP. The hyperfine interaction in organic RPs induces transitions between the RP's spin states (one singlet S and three triplet states T_+, T_0, and T_-). In an external magnetic field the Zeeman splitting removes the degeneracy of two triplet levels (T_+ and T_-) with the singlet state, thus reducing singlet-triplet mixing (*2*). The saturation field of such effects is determined by the magnitude of the hyperfine interaction, which is ~0.005 T (1 T = 10^4 gauss) in organic RPs. This field range also determines the time scale for these effects to evolve, which is ~10 ns (*3, 4*). In this regime, magnetic field effects have been successfully used to separate spin processes and elementary chemical processes such as electron transfer (ET) and bond formation (*5–7*).

Here, we report an ultrafast magnetic field effect on the recombination of an RP containing a transition metal component that occurs in less than 10 ps in fields of several teslas. Using femtosecond pump-probe spectroscopy and an optical superconducting magnet (*8*) we investigated the RP generated from ethylferrocene (Fc) and oxazine 1 in its first excited singlet state ($^1Ox^{+*}$) in acetonitrile solution (*9*) at 298 K. Analogous to the closely related *N,N*-dimethylmethylferrocene–methylene blue photo-redox system (*10*), $^1Ox^{+*}$ accepts an electron from the neutral Fc. At high concentrations of Fc, the forward ET measured in stimulated emission from $^1Ox^{+*}$ is ultrafast (time constant ~200 fs) and follows essentially monoexponential kinetics. For energetic reasons the resulting RP $(Ox^{\bullet}\cdot\cdot\cdot Fc^{+\bullet})$ can only recombine to form the singlet ground states of the reactants.

The recombination monitored by the recovery of Ox^+ shows multiexponential kinetics in zero field (Fig. 1). The dominant process proceeds with a time constant of ~1 ps, a sizeable fraction decays with a time constant of ~13 ps, and a small, long-lived contribution has a characteristic time of ~130 ps that is responsible for the offset in Fig. 1. This rather complex behavior can be attributed to the transition metal component $(Fc^{+\bullet})$ in the RP. Replacing it by the cation of *N,N*-dimethylaniline results in a nearly monoexponential decay independent of magnetic fields (Fig. 2).

Magnetic fields of several teslas affect the recombination of the $Fc^{+\bullet}$-containing RP (Fig. 1). The general effect at short times is to slow down the recombination. With increasing magnetic field the effect increases and its onset moves to earlier times. For the largest field applied, the magnetic field effect reaches its maximum at 2 ps. At longer times a cross-over behavior is observed, implying that, in contrast to the behavior at short times, increasing magnetic fields accelerate the recombination.

Qualitatively, the observed effects are accounted for by the following reaction scheme:

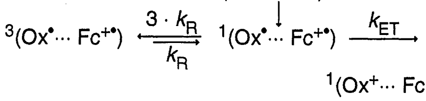

$$\begin{tikzcd} & {^1(Ox^{+*}\cdots Fc)} \arrow[d] & \\ {^3(Ox^{\bullet}\cdots Fc^{+\bullet})} \arrow[r, shift left, leftarrow, "3\cdot k_R"] \arrow[r, shift right, "k_R"'] & {^1(Ox^{\bullet}\cdots Fc^{+\bullet})} \arrow[r, "k_{ET}"] & {} \\ & & {^1(Ox^{+}\cdots Fc)} \end{tikzcd}$$

Generation of the RP by the singlet precursor $^1(Ox^{+*}\cdot\cdot\cdot Fc)$ yields a singlet-correlated RP $^1(Ox^{\bullet}\cdot\cdot\cdot Fc^{+\bullet})$, which can recombine (rate constant k_{ET}) to form the ground-state reactants. Alternatively, the RP may

---

P. Gilch, F. Pöllinger-Dammer, C. Musewald, M. E. Michel-Beyerle, Institut für Physikalische und Theoretische Chemie, Technische Universität München, D-85748 Garching, Germany. U. E. Steiner, Fakultät für Chemie, Universität Konstanz, D-78434 Konstanz, Germany.

*To whom correspondence should be addressed. E-mail: mibe@zentrum.phys.chemie.tu-muenchen.de